ChemComm

COMMUNICATION

View Article Online
View Journal | View Issue

Check for updates

Cite this: *Chem. Commun.*, 2024, **60**, 8549

Received 8th May 2024,
Accepted 7th July 2024

DOI: 10.1039/d4cc02241f

rsc.li/chemcomm

Open Access Article. Published on 08 July 2024. Downloaded on 12/26/2025 10:01:16 AM.
This article is licensed under a Creative Commons Attribution 3.0 Unported Licence.

A dinuclear nickel peroxycarbonate complex: CO_2 addition promotes H_2O_2 release†

Hayley L. Lillo and Joshua A. Buss *

Nickel coordination compounds featuring Ni–O bonds are key structural motifs in both bioinorganic and synthetic chemistries. They serve as precursors for organic substrate oxidation and are commonly invoked intermediates in water oxidation and oxygen reduction schemes. Herein, we disclose a series of well-defined dinuclear nickel complexes that, upon treatment with CO_2 and H_2O_2, afford the first nickel-bound peroxycarbonate. This unprecedented nickel–oxygen intermediate is stabilized by hydrogen bonding templated across the bimetallic core. Contrasting copper and iron analogues, the nickel peroxycarbonate reversibly dissociates H_2O_2, a process that is shown to be accelerated by exogenous CO_2.

The ubiquity of Cu, Fe, and Mn enzymes has led to extensive studies interrogating metal-oxygen intermediates of mono- and bimetallic complexes of these ions.[1] In contrast, Ni is generally employed by Nature for C_1 conversion chemistry,[2] but has recently received attention with respect to oxidation reactivity given its role in the active sites of superoxide dismutase (NiSOD; Fig. 1A)[3] and dioxygenase enzymes.[4] Ni(II) complexes are typically inert to dioxygen, however modifications to the supporting ligand(s) have been demonstrated to override this tendency.[5] Even so, the vast majority of nickel–oxygen complexes are accessed *via* addition of strong oxidants, including H_2O_2, peroxyacids, and alkylperoxides.[6] Continued preparation and study of new classes of nickel–oxygen intermediates is critical to elucidating the chemistry of nickel metalloenzymes, informing fundamental mechanisms in synthetic oxidation catalysis, and providing a basis for comparison to copper and iron homologs.[6c]

Given the high electronegativity of Ni, its low oxophilicity, and O(π)/Ni(d) repulsions, nickel–oxygen species can demonstrate potent oxidative reactivity.[7] Mononuclear nickel oxidants—generated from the treatment of Ni(II) precursors with peroxyacids—are capable of oxidizing unactivated aliphatic C–H bonds, yet the nature of the active oxidant remains unknown.[8] Tyrosinase-like Ni^{III}-μ(O)$_2$-Ni^{III} diamond cores are competent for intramolecular aliphatic[9] and aromatic[10] C–H oxygenation, ultimately sourcing the oxidizing equivalents from hydrogen peroxide (H_2O_2). They are likewise proposed to be the active oxidants in catalytic aromatic hydroxylation protocols.[1a,11] Recently, this has been scrutinized;[12] more exotic nickel–oxygen species have been reported under similar reaction conditions and cannot be strictly ruled out as reaction-relevant intermediates (Fig. 1B).[9,13]

Given that many mechanistic proposals rely on self-assembly of monometallic precursors to dinuclear nickel–oxygen species, our lab has targeted well-defined bimetallic model systems

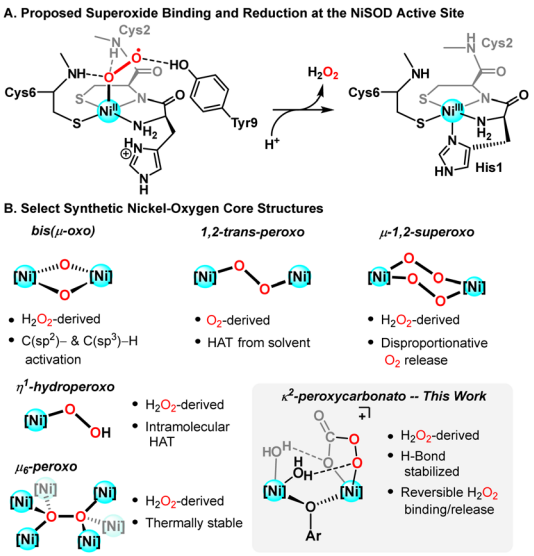

Fig. 1 Proposed mechanism for bioinorganic superoxide reduction to H_2O_2 (A) and representative examples of the diverse nickel–oxygen intermediates accessed synthetically *via* both O_2 activation and H_2O_2/base addition (B).

Willard Henry Dow Laboratory, Department of Chemistry, University of Michigan 930 N. University Avenue, Ann Arbor, MI 48109, USA. E-mail: jbuss@umich.edu

† Electronic supplementary information (ESI) available. CCDC 2348000–2348003. For ESI and crystallographic data in CIF or other electronic format see DOI: https://doi.org/10.1039/d4cc02241f

Open Access Article. Published on 08 July 2024. Downloaded on 12/26/2025 10:01:16 AM.
This article is licensed under a Creative Commons Attribution 3.0 Unported Licence.

supported by a bicompartmental ligand scaffold. Herein, we describe the synthesis of a series of multinuclear nickel complexes that serve as precursors for base-free H_2O_2 activation chemistry. These Ni(II) compounds were found to readily react with carbon dioxide (CO_2), affording a dinickel complex bridged by κ^2-bicarbonate linkages. The CO_2 in these ligands plays a key role in subsequent H_2O_2 reactivity, yielding the first structurally characterized bimetallic peroxycarbonate complex, $[LNi_2(O_2CO_2)(H_2O)_2]^+$. Contrasting previously reported peroxycarbonates,[14] $[LNi_2(O_2CO_2)(H_2O)_2]^+$ releases H_2O_2 when warmed to 0 °C. In addition to expanding the library of characterized nickel–oxygen intermediates (Fig. 1B), this work lends credence to proposed peroxyacid adducts that are relevant to nickel-mediated alkane and alkene oxidations.[8a,c,d]

Treating lithium phenolate pro-ligand, **LiL**, with two equiv. of $Ni(OTf)_2$, generates a dinickel complex[15] featuring both inner- (^{19}F δ = 0.81 ppm) and outer-sphere (^{19}F δ = –74.42 ppm) triflate anions. The nickel(II) centres afford sharp paramagentically shifted resonances by ^1H NMR spectroscopy, a fingerprint correlated to the bis(triflate) cation $[LNi_2(OTf)_2]^+$ (Scheme 1), *via* complementary single crystal X-ray diffraction (SCXRD) analysis. μ-OH ligands are purported intermediates and/or precursors in H_2O_2-mediated oxidation chemistry;[16] these groups were targeted *via* treatment of $[LNi_2(OTf)_2]^+$ with NaOH. Under anaerobic conditions, addition of base results in generation of a tetranuclear complex with μ-OH ligands linking two distinct LNi_2 motifs, the formulation of which was corroborated as $[L_2Ni_4(OH)_4]^{2+}$ by SCXRD. The four metal ions adopt a roughly tetrahedral arrangement (τ_4 = 0.97),[17] with bridging hydroxide and aryloxide ligands capping each of the six edges. The Ni–Ni distances across the aryloxide bridges are slightly elongated (3.90 Å) relative to those spanned by the hydroxide ligands (3.75 Å), suggesting that the intermolecular μ-hydroxo is more accessible with the semi-rigid dinucleating scaffold. When the same reaction is performed open to air, a distinct tetranickel complex results, with two bridging carbonate and two aquo ligands, $[L_2Ni_4(CO_3)_2(H_2O)_2]^{2+}$, *via* the uptake of CO_2 from ambient air (Scheme 1). All four Ni(II) centres remain six-coordinate with C_2 symmetry and μ-κ^2O,O:κO carbonate binding. The solid-state structure of this species highlights expansion of the inter-nickel distances between the two bimetallic units (Ni···$Ni_{ave.}$ = 4.96 Å), and distinct Ni–Ni contacts within the two bicompartmental chelates, with the κ^2-carbanato moieties enforcing a more compact Ni_2 spacing (*viz.* 3.45 *vs.* 3.81 Å). The solid state asymmetry observed for $[L_2Ni_4(CO_3)_2(H_2O)_2]^{2+}$ is affirmed by the solution spectroscopy, and electrospray ionization mass spectrometry (ESI-MS) shows parent ion peaks consistent with both tetranuclear units, $[L_2Ni_4(OH)_4]^{2+}$ and $[L_2Ni_4(CO_3)_2(H_2O)_2]^{2+}$.

Whereas solutions of $[L_2Ni_4(OH)_4]^{2+}$ prove air-stable, they readily react with concentrated CO_2 (1 atm) to generate a new species, as indicated by a slight blue shift in the UV-visible spectrum (Fig. 2, left) and a distinct paramagnetically shifted signature in the ^1H NMR spectrum.[18] The same spectral features are reproduced when CO_2 (1 atm) is added to $[L_2Ni_4(CO_3)_2(H_2O)_2]^{2+}$. Vibrational spectroscopy shows a sharp carbonyl stretch at 1687 cm^{-1} that is sensitive to $^{13}CO_2$ isotopic labelling (Fig. 2, right), most consistent with a terminal (bi)carbonate assignment.[14h] Whereas this reaction product has eluded characterization in the solid state, ESI-MS of reactions stemming from the treatment of either precursor with $^{12/13}CO_2$ corroborates generation of a bis(bicarbonate) cation, $[LNi_2(CO_3H)_2]^+$, the dinuclear nature of which is further supported by DOSY NMR experiments (Scheme 1).

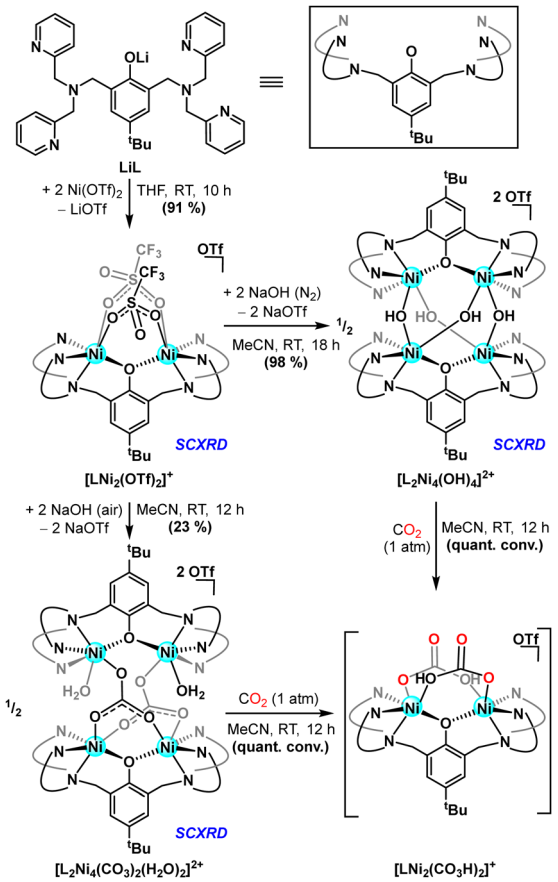

Scheme 1 Synthesis of well-defined multinuclear nickel hydroxide complexes and subsequent reactivity with carbon dioxide.

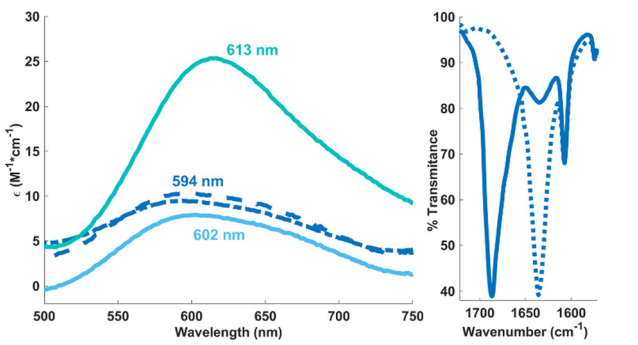

Fig. 2 Electronic absorption spectra evidencing conversion of $[L_2Ni_4(OH)_4]^{2+}$ (—) and $[L_2Ni_4(CO_3)_2(H_2O)_2]^{2+}$ (—) to $[LNi_2(CO_3H)_2]^+$ (— — & — -, respectively) in MeCN solution (left). Solution IR spectra (MeCN) corroborating isotopic sensitivity of the bicarbonate (^{12}C —; ^{13}C ---) carbonyl stretch (right).

 This journal is © The Royal Society of Chemistry 2024

Open Access Article. Published on 08 July 2024. Downloaded on 12/26/2025 10:01:16 AM.
This article is licensed under a Creative Commons Attribution 3.0 Unported Licence.

As an entry point to oxidative chemistry, we pursued H_2O_2 addition to these multinuclear Brønsted-basic nickel species. Peroxycarbonate ligands are shown to form from both CO_2 addition to reactive metal peroxo species[14b,d,f–k] and H_2O_2 insertion into metal carbonatos.[14a] Treating $[L_2Ni_4(CO_3)_2(H_2O)_2]^{2+}$ or $[LNi_2(CO_3H)_2]^+$ with excess aqueous H_2O_2 (50 wt%) at −30 °C resulted in an immediate colour change to pale purple. Low temperature ^{1}H NMR spectroscopy supported the formation of a mixture of paramagnetic species; cleaner reactivity to a single major product was observed when the oxidant addition was carried out in the presence of exogenous CO_2. Crystalline purple plates were formed when Et_2O/MeCN mixtures of this new product were maintained at low temperature (−17 °C). SCXRD analysis revealed generation of a dinuclear peroxycarbonate complex, $[LNi_2(O_2CO_2)(H_2O)_2]^+$ (Fig. 3); the first nickel peroxycarbonate and the first structurally characterized bimetallic example.

Contrasting what was proposed for dicopper complexes on a similar phenolate-bridged ancillary ligand,[14h] the present dinickel peroxycarbonate shows preferential binding to a single Ni centre (Fig. 3). The metrical parameters highlight that the O_2CO_2-bound Ni ion in $[LNi_2(O_2CO_2)(H_2O)_2]^+$ adopts a distorted octahedral coordination environment, with peroxycarbonate bond lengths similar to Suzuki's related monometallic Fe analogue.[14e] The O–O bond is slightly elongated in the present case (*cf.* 1.466(6) *vs.* 1.455(5) Å) and more closely matches that of the recently reported peroxybicarbonate anion (1.469(2) Å).[19] The second nickel centre in $[LNi_2(O_2CO_2)(H_2O)_2]^+$ is likewise pseudo-octahedral with two water molecules completing the coordination sphere. A striking feature of the solid-state structure is the orientation and proximity of the aquo ligands to the formally anionic oxygen atoms of the peroxycarbonate, which are well within the range of H-bonding contacts ($OH_2\cdots O_{ave.}$ = 2.682(5) Å). H-bonding is a proven strategy for stabilizing reactive metal-oxygen species;[20] we hypothesize that nickel templated intramolecular H-bonding imbues added stability to the peroxycarbonate moiety in the present system.

The reported reactivity of base-metal peroxycarbonate complexes varies, with documented examples of both O–O bond scission[14a,c] and thermal disproportionation to liberate O_2.[14h] Moreover, peroxycarbonate complexes have been shown to be competent oxidants in their own right, demonstrating O-atom[14a,b,e–h] and H-atom transfer[14a,f] reactivity. In light of this precedent, we were keen to explore the thermal (in)stability of $[LNi_2(O_2CO_2)(H_2O)_2]^+$, which demonstrated relatively slow conversion to $[L_2Ni_4(CO_3)_2(H_2O)_2]^{2+}$ in MeCN solution at 0 °C ($t_{1/2}$ *ca.* 40 min.). This is markedly different from Karlin's dicopper analogue, which reacts rapidly *via* thermal disproportionation at temperatures as low as −50 °C,[14h] a distinction attributed to the intramolecular H-bonds (*vide supra*). A balanced reaction for formation of $[L_2Ni_4(CO_3)_2(H_2O)_2]^{2+}$ necessitates the loss of H_2O_2—efforts to spectroscopically identify/quantify H_2O_2 were unsuccessful, but reactivity probes with phosphine reagents corroborated nearly quantitative peroxide release (92%; Fig. S21, ESI†).§ In this way, $[LNi_2(O_2CO_2)(H_2O)_2]^+$ demonstrates novel reactivity for this ligand motif, acting as a reservoir for H_2O_2.

We next sought to explore the potential of $[LNi_2(O_2CO_2)(H_2O)_2]^+$ to serve as a *bona fide* oxidant *via* low-temperature reactions with various substrates. Kinetic assays at 0 °C, under pseudo first-order conditions, displayed non-integer rate laws (Fig. 4● and ●) for two electronically differentiated phosphines. These results are more consistent with reversible H_2O_2 binding than the direct reaction of PR_3 with $[LNi_2(O_2CO_2)(H_2O)_2]^+$. A kinetic regime in which H_2O_2 binding to form $[LNi_2(O_2CO_2)(H_2O)_2]^+$ (Fig. 3, k_{-1}) is rate competitive with phosphine oxidation (k_2) rationalizes the observed reaction profiles.¶ To further bolster this hypothesis, the rate of carbonate formation from $[LNi_2(O_2CO_2)(H_2O)_2]^+$ in the presence (×) and absence (×) of H_2O_2 was likewise investigated. The zero-order dependence on Ni observed for formation of $[L_2Ni_4(CO_3)_2(H_2O)_2]^{2+}$ supports rate determining H_2O_2 release (rather than dimerization), and addition of exogenous H_2O_2 suppresses conversion (Fig. 4× and ×, respectively). A comparison of three additional substrates (Fig. 3, inset) demonstrated no significant difference in reactivity relative to hydrogen peroxide controls, further supporting $[LNi_2(O_2CO_2)(H_2O)_2]^+$ acts as a storehouse for H_2O_2.

Reaction atmosphere—N_2 *vs.* CO_2 *vs.* air—has been shown to play a role in peroxycarbonate reactivity.[14a] Under CO_2, the

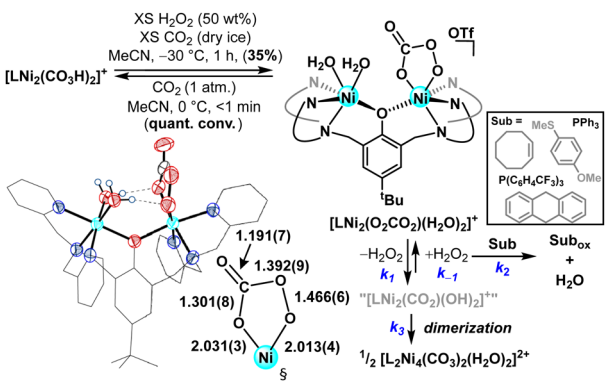

Fig. 3 Synthesis, solid-state structure,‡ and reactivity of a nickel peroxycarbonate complex. Bond metrics are reported in angstroms. Substrate oxidations were conducted at 0 °C for 4 hrs in either MeCN or MeCN/DCM.

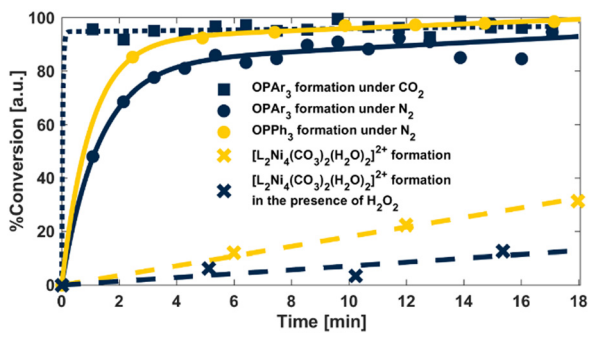

Fig. 4 Reaction kinetics tracking $[LNi_2(O_2CO_2)(H_2O)_2]^+$ reactivity under conditions outlined in the accompanying legend. Ar = tris(4-trifluoromethylphenyl).

Open Access Article. Published on 08 July 2024. Downloaded on 12/26/2025 10:01:16 AM.
This article is licensed under a Creative Commons Attribution 3.0 Unported Licence.

decomposition of $[LNi_2(O_2CO_2)(H_2O)_2]^+$ is immediate, even at low temperature (thawing MeCN), quantitatively furnishing bicarbonate complex $[LNi_2(CO_3H)_2]^+$. Again, this chemistry proceeds *via* the release of H_2O_2 with concomitant CO_2 uptake. This reversible sequestration of H_2O_2 at a base-metal-bound peroxycarbonate is unprecedented, differentiating the present Ni reactivity from that of both its Fe[14a,c] and Cu[14g] congeners. Subsequent chemical steps—dimerization to form $[L_2Ni_4(CO_3)_2(H_2O)_2]^{2+}$, substrate oxidation, or CO_2 addition (generating $[LNi_2(CO_3H)_2]^+$)—serve to drive the equilibrium toward exhaustive H_2O_2 release.

In summary, well-defined dinuclear nickel complexes have been accessed by employing a phenolate-bridged bicompartmental ligand scaffold. Hydroxide installation results in highly Lewis basic moieties that favour intermolecular bridging ($[L_2Ni_4(OH)_4]^{2+}$) or CO_2 uptake ($[L_2Ni_4(CO_3)_2(H_2O)_2]^{2+}$). Ensuing hydrogen peroxide chemistry affords the first reported example of a nickel peroxycarbonate complex, the stability of which is attributed to metal-templated intramolecular H-bonding interactions. Unlike previously reported metal peroxycarbonates,[14] $[LNi_2(O_2CO_2)(H_2O)_2]^+$ reacts *via* reversible H_2O_2 release, as established by kinetics assays. H_2O_2 dissociation is shown to be driven by CO_2 addition, accelerating oxidant release. Compounding ambiguity regarding the exact nature of reactive nickel–oxygen intermediates accessed from H_2O_2 and base (*cf.* Fig. 1B), this work demonstrates that CO_2 may likewise play a non-innocent role in altering the nickel speciation. Further studies investigating the fundamental chemistry of multinuclear nickel precursors with myriad catalysis-relevant oxidants are underway in our laboratory.

This work was supported by the University of Michigan and the NSF (XRD Instrumentation–CHE-0840456). We thank Dr. Eugenio Alvarado for NMR spectroscopy expertise, Drs. Jeff Kampf and Fengrui Qu for assistance with SCXRD and Claire R. Patterson for XRD data of $[LNi_2(OTf)_2]^+$. Roy Wentz aided in the design and fabrication of custom glassware and the Szymczak lab shared instrumentation that made this work possible.

Data availability

The data supporting this article have been included as part of the ESI.† Crystallographic data have been deposited in the CCDC (2348000–2348003)—**https://www.ccdc.cam.ac.uk/structures**.

Conflicts of interest

There are no conflicts to declare.

Notes and references

‡ Thermal anisotropic displacement ellipsoids are shown at the 50% probability level; non-aquo hydrogen atoms and the triflate counterion are omitted for clarity. The hydrocarbyl ligand backbone is depicted as a wireframe for simplicity.

§ Control reactions of $[L_2Ni_4(CO_3)_2(H_2O)_2]^{2+}$ and phosphine under O_2 did not result in any detectable oxidation to phosphine oxide on the timescale of these experiments.

¶ The difference in phosphine oxidation rate is insufficient to rule out direct reaction of the phosphine with $[LNi_2(O_2CO_2)(H_2O)_2]^+$; however, in totality, the data are inconsistent with this mechanism.

1 (*a*) L. Vicens, *et al.*, *ACS Catal.*, 2020, **10**, 8611; (*b*) L. Que and W. B. Tolman, *Nature*, 2008, **455**, 333; (*c*) E. A. Lewis and W. B. Tolman, *Chem. Rev.*, 2004, **104**, 1047; (*d*) L. M. Mirica, *et al.*, *Chem. Rev.*, 2004, **104**, 1013.
2 S. W. Ragsdale, *Crit. Rev. Biochem. Mol. Biol.*, 2004, **39**, 165.
3 (*a*) D. P. Barondeau, *et al.*, *Biochem.*, 2004, **43**, 8038; (*b*) J. Wuerges, *et al.*, *Proc. Natl. Acad. Sci. U. S. A.*, 2004, **101**, 8569.
4 (*a*) J.-H. Jeoung, *et al.*, *Angew. Chem., Int. Ed.*, 2016, **55**, 3281; (*b*) T. C. Pochapsky, *et al.*, *Nat. Struct. Bio.*, 2002, **9**, 966.
5 (*a*) D. M. Beagan, *et al.*, *J. Am. Chem. Soc.*, 2024, **146**, 12375; (*b*) A. J. McNeece, *et al.*, *J. Am. Chem. Soc.*, 2020, **142**, 10824; (*c*) N. Zhao, *et al.*, *J. Am. Chem. Soc.*, 2020, **142**, 21634; (*d*) P.-C. Duan, *et al.*, *J. Am. Chem. Soc.*, 2018, **140**, 4929.
6 (*a*) H. Noh and J. Cho, *Coord. Chem. Rev.*, 2019, **382**, 126; (*b*) T. Corona and A. Company, *Chem. Eur. J.*, 2016, **22**, 13422; (*c*) M. R. Halvagar, *et al.*, 3.17-Small Molecule Models: Cu, Ni, Co, in *Comprehensive Inorganic Chemistry II*, ed. J. Reedijk and K. Poeppelmeier, 2nd edn, Elsevier, Amsterdam, 2013, p. 455.
7 J. R. Winkler and H. B. Gray, in *Molecular Electronic Structures of Transition Metal Complexes I*, ed. D. M. P. Mingos, P. Day and J. P. Dahl, Springer, Berlin, Heidelberg, 2012, 17.
8 (*a*) J. Nakazawa, *et al.*, *J. Am. Chem. Soc.*, 2013, **135**, 6010; (*b*) S. Hikichi, *et al.*, *Dalton Trans.*, 2013, **42**, 3346; (*c*) T. Nagataki, *et al.*, *Dalton Trans.*, 2007, 1120; (*d*) T. Nagataki, *et al.*, *Chem. Commun.*, 2006, 4016.
9 (*a*) J. Cho, *et al.*, *Inorg. Chem.*, 2006, **45**, 2873; (*b*) S. Itoh, *et al.*, *J. Am. Chem. Soc.*, 2001, **123**, 11168; (*c*) K. Shiren, *et al.*, *J. Am. Chem. Soc.*, 2000, **122**, 254.
10 (*a*) T. Tano, *et al.*, *Bull. Chem. Soc. Jpn.*, 2010, **83**, 530; (*b*) K. Honda, *et al.*, *Angew. Chem., Int. Ed.*, 2009, **48**, 3304; (*c*) A. Kunishita, *et al.*, *Inorg. Chem.*, 2009, **48**, 4997.
11 (*a*) S. Muthuramalingam, *et al.*, *Catal. Sci. Tech.*, 2019, **9**, 5991; (*b*) Y. Morimoto, *et al.*, *J. Am. Chem. Soc.*, 2015, **137**, 5867.
12 K. Farshadfar and K. Laasonen, *Inorg. Chem.*, 2024, **63**, 5509.
13 (*a*) M. T. Kieber-Emmons, *et al.*, *J. Am. Chem. Soc.*, 2006, **128**, 14230; (*b*) E. J. Brown, *et al.*, *Angew. Chem., Int. Ed.*, 2005, **44**, 1392; (*c*) S. Hikichi, *et al.*, *J. Am. Chem. Soc.*, 1998, **120**, 10567.
14 (*a*) T. Tsugawa, *et al.*, *Chem. Lett.*, 2015, **44**, 330; (*b*) G. Meier and T. Braun, *Angew. Chem., Int. Ed.*, 2012, **51**, 12564; (*c*) H. Furutachi, *et al.*, *J. Am. Chem. Soc.*, 2005, **127**, 4550; (*d*) M. Yamashita, *et al.*, *J. Am. Chem. Soc.*, 2005, **127**, 7294; (*e*) K. Hashimoto, *et al.*, *Angew. Chem., Int. Ed.*, 2002, **41**, 1202; (*f*) M. Aresta, *et al.*, *Inorg. Chem.*, 1996, **35**, 4254; (*g*) I. Sanyal, *et al.*, *J. Am. Chem. Soc.*, 1993, **115**, 11259; (*h*) P. P. Paul, *et al.*, *J. Am. Chem. Soc.*, 1991, **113**, 5322; (*i*) M. Schappacher and R. Weiss, *Inorg. Chem.*, 1987, **26**, 1189; (*j*) L. Dahlenburg and C. Prengel, *J. Organomet. Chem.*, 1986, **308**, 63; (*k*) P. J. Hayward, *et al.*, *J. Chem. Soc. D*, 1969, 987b.
15 (*a*) H. T. Zhang, *et al.*, *Angew. Chem., Int. Ed.*, 2023, **62**, e202218859; (*b*) S. S. Massoud, *et al.*, *Dalton Trans.*, 2015, **44**, 2110; (*c*) Y. Gultneh, *et al.*, *Polyhedron*, 1998, **17**, 3351.
16 A. Rajeev, *et al.*, *ACS Catal.*, 2022, **12**, 9953.
17 L. Yang, *et al.*, *Dalton Trans.*, 2007, 955.
18 D. Huang, *et al.*, *Proc. Natl. Acad. Sci. U. S. A.*, 2011, **108**, 1222.
19 Z. Yan, *et al.*, *J. Am. Chem. Soc.*, 2023, **145**, 22213.
20 (*a*) E. W. Dahl, *et al.*, *Chem. Commun.*, 2018, **54**, 892; (*b*) E. W. Dahl, *et al.*, *J. Am. Chem. Soc.*, 2018, **140**, 10075; (*c*) C. L. Ford, *et al.*, *Science*, 2016, **354**, 741; (*d*) A. S. Borovik, *Acc. Chem. Res.*, 2005, **38**, 54; (*e*) C. E. MacBeth, *et al.*, *Science*, 2000, **289**, 938.

 This journal is © The Royal Society of Chemistry 2024